Materials Horizons

Accepted Manuscript

ROYAL SOCIETY OF CHEMISTRY

rsc.li/materials-horizons

Journal Name

Materials Horizons

Dynamic Article Links ►

Cite this: DOI: 10.1039/c0xx00000x

www.rsc.org/xxxxxx

ARTICLE TYPE

Fluorescent Quantum Dots Derived from PEDOT and their Applications for Optical Imaging and Sensing

Kenath Priyanka Prasad[a], Yun Chen[a], Mahasin Alam Sk[a], Aung Than[a], Yue Wang[b], Hangdong Sun[b], Kok-Hwa Lim[a], Xiaochen Dong[c] and Peng Chen[a]*

Received (in XXX, XXX) Xth XXXXXXXXX 20XX, Accepted Xth XXXXXXXXX 20XX
DOI: 10.1039/b000000x

We herein demonstrate a facile and general approach to synthesize novel polymer quantum dots (QDs) derived from non-fluorescent poly(3,4-ethylenedioxythiophene) (PEDOT). Such PEDOT-QD is of molecular size and exhibits excellent photostability, two-photon excitation property, and biocompatibility. Furthermore, we demonstrate the use of this new type of fluorescent reporter for cellular imaging, sensitive and specific optical detection of mercury ions. The synthetic route demonstrated here can be easily modified (e.g., using different polymer precursors, ionic liquids for polymerization, solvents for exfoliation) to produce different types of polymer QDs with various interesting properties.

Introduction

Lighting up the perplexing and dynamic biological processes conventionally relies on organic fluorophores (fluorescent proteins and dyes). But they intrinsically suffer from rapid photo-bleaching which makes long-term real-time imaging difficult. Semiconductor quantum dots (semi-QDs) with high photo-stability have thus been regarded as the alternative fluorescent reporters[1-3]. These semi-QDs, however, exhibit several innate limitations, including cytotoxicity due to leaching of heavy metal ions, blinking which makes single-molecule tracking challenging and too-large a size which alters the functions / dynamics of the targeted molecules and creates non-physiological clusters while interacting with multiple target molecules. More recently, graphene quantum dots (GQDs) have demonstrated the potentials for real-time molecular imaging in live cells owing to its good photostability, small size, and biocompatibility[4, 5]. Both semi-QDs and GQDs have demonstrated potentials for sensitive detection of biomolecules or chemicals[6-9]. But these synthetic fluorophores are still not perfectly photo-stable, and usually require nontrivial synthesis or purification processes.

It has been recently demonstrated that QDs derived from fluorescent semiconducting polymers (pQDs) show super photo-stability, together with other merits including high brightness, tunable photoluminescence properties, non-blinking property, and biocompatibility[10-15]. Nevertheless, these polymer nanoparticles are sometimes large in size (up to 100 nm). And the synthetic routes are usually tedious. Herein, we report a facile approach to synthesize a new type of pQDs derived from non-fluorescent poly(3,4-ethylenedioxythiophene) (PEDOT), which exhibit molecular size, remarkable photo-stability, two-photo excitation property, and good biocompatibility. The optical properties of PEDOT-QDs are consistent with the theoretical calculations. Furthermore, the applications of this novel PEDOT-QD for cellular imaging and optical sensing of mercury ions (Hg^{2+}) are demonstrated.

Experimental Section

Preparation of fibrous PEDOT film. 3,4-ethylenedioxylthiophene(EDOT) monomer, ionic liquid (1-n-Butyl-3-methylimidazolium tetrafluoroborate - $BMIMBF_4$) and N,N-Dimethylformide (DMF) were purchased from Sigma Aldrich. With 0.1 M EDOT monomer in the ionic liquid, PEDOT film was polymerized on an ITO working electrode held at the constant potential of 1 V for 3 h. An electrochemical workstation (CHI 660D) was used for polymerization, with a three-electrode configuration consisting of a platinum plate counter electrode, silver wire reference electrode and an ITO working electrode. Thorough washing to eliminate excess ionic liquid and unreacted monomers and overnight drying in a vacuum oven at 27 ^{0}C followed polymerization.

Preparation of PEDOT-QDs. The polymer film was then gently scraped off the ITO electrode and suspended in DMF solvent (1 mg/ml), followed by ultrasonication (Branson 2510; 1.1 A, 230 W) at 27 ^{0}C for 4 h. After centrifugation at 10,000 rpm for 30 min, the supernatant was collected. This was repeated for 5 times to obtain the dispersion of PEDOT-QDs in DMF, which was subsequently filtered using a WHATMAN 0.2 µm PTFE filter. To re-suspend PEDOT-QDs in distilled water, DMF was completely extracted using rotary evaporation at 80 ^{0}C, and distilled water was added to the dried QD aggregates. The solution was then ultra-filtered (molecular cut-off weight of 3 kDa) to remove the aggregates. PEDOT-QD suspensions in both DMF and water are highly stable (lasting for months without apparent aggregation).

Characterizations. The samples were examined by field emission scanning electron microscopy (FESEM, JMS-6700F), atomic force microscopy (MFP-3D AFM microscope, Asylum research), raman spectroscopy (WITec CRM200 using 633 nm laser), high-resolution transmission electron microscopy (HRTEM, JEOL 2010), X-ray photoelectron spectroscopy (ESCALAB MK-II), X-ray diffraction (Bruker D8 Avance

diffractometer using Cu Kα radiation) and Fourier transform infrared spectroscopy (Perkin Elmer FTIR Spectrum GX 69233). The UV-vis absorption and photoluminescence performance of QDs was characterized by UV-2450 spectrophotometer (Shimadzu), and LS-55 fluorescence spectrometer (PerkinElmer), respectively.

Cell imaging. The PC12 cells (American Type Culture Collection) were cultured in Dulbecco's modified Eagle's medium (DMEM, Gibco) supplemented with 10% (v/v) fetal bovine serum (Gibco) and 1% penicillin–streptomycin, at 37 °C under a humidified atmosphere containing 5% CO_2 and 95% air. Cells were incubated with 76.6 μg/ml blue PEDOT-QDs (dispersed in water) or 5.5 μg/ml green PEDOT-QDs (dispersed in DMF) for 24 h before imaging with a confocal laser scanning microscope (LSM 510 Meta, Carl Zeiss GMbH, Germany). The blue (or green) QDs were excited at 405 (or 488) nm and detected with an emission filter <480 nm (or >520 nm).

Optical detection of Hg^{2+} ions. The photoluminescence of PEDOT-QDs (1 mg/ml in DMF was diluted by 5 times in distilled water) was measured before and after adding various metal salts at defined concentrations, including mercury(II) perchlorate, lead(II) nitrate, zinc Nitratehexahydrate, cadmium chloride, cesium chloride, magnesium sulphate, cobalt nitratehexahydrate, nickel nitratehexahydrate, manganese nitratetetrahydrate, gold(III) chloride trihydrate and potassium chloride

Results & Discussion

Synthesis and morphology of PEDOT-QDs

As schematically illustrated (Scheme 1), EDOT monomers are electro-polymerized in an ionic liquid ($BMIMBF_4$). Field-effect scanning electron microscopy (FESEM) reveals that a film of polymerized EDOTs (PEDOT) consequently forms on the ITO electrode (Figure 1a). On the film, ultra-long wires and roots of outgrowing wires can be observed (bright dots and lines in Figure 1a). A closer inspection shows that the film consists of dense interwoven fibers (inset in Figure 1a). The fibrous PEDOT film is then sonicated in DMF solvent, producing a yellow solution with well-dispersed PEDOT-QDs exfoliated from the film (Scheme 1). As observed from atomic force microscopy (AFM), the PEDOT-QDs exhibit quantized thickness (Figure 1b, c) with the average thickness of ~0.40 nm (+/- 0.17, n = 152) and a quantal step of ~0.21 nm (corresponding to the thickness of the single PEDOT chain[16]). This suggests that PEDOT-QDs range from single to a-few layers. High-resolution transmission electron microscopy (HRTEM) shows that PEDOT-QDs are uniform in diameter (~2.3 +/- 0.36 nm, n = 172) (Figure 1d, e). The diffraction pattern indicates that the QDs possess a certain degree of crystallinity (lower inset in Figure 1d). Indeed, well-defined crystal lattice can be resolved from some QDs under high-resolution TEM (upper inset in Figure 1d). Consistent with a previous study[17], the observed lattice spacing of 3.4 Å corresponds to the characteristic face-to-face distance (010) of the rigid PEDOT polymer, similar to graphite. Therefore, it appears that the disc-like QDs are mechanically chopped by sonication from the crystalline PEDOT polymer chain. Figure 1f presents the gel-electrophoresis result of PEDOT-QD sample in comparison with protein markers. The bright field and fluorescence gel images show a narrow band of PEDOT-QDs indicating that they have a uniform size distribution and a molecular weight <10 kDa which is comparable to a single small protein.

Spectroscopic characterization of PEDOT-QDs

X-ray photoelectron spectroscopy (XPS) spectra of both PEDOT-film and PEDOT-QDs show the characteristic S2s (228 eV), S2p (163 eV), C1s (283 eV) and O1s (531 eV) peaks from PEDOT (Figure 2a) [18,19]. The spectrum of PEDOT-film also exhibits B1s (193 eV), N1s (401 eV), and F1s (685 eV) peaks resulted from the remaining ionic liquid ($BMIMBF_4$) from the polymerization process[20]. The B1s and F1s peaks diminish in the XPS spectrum of PEDOT-QDs while the N1s peak is significantly reduced. Deconvolution of the high resolution XPS spectra of C1s (Figure 2b) and S2p (Figure 2c) indicate the existence of the (C=C) sp^2, (C-C) sp^3, C-S, C-O, $S2p_{3/2}$, and $S2p_{1/2}$ peaks characteristic to PEDOT, and small C-N and C=N peaks characteristic to $[BMIM]^+$ [9,21]. The small amount of association of the nitrogen-containing ionic liquid is also confirmed by the high-resolution N1s spectrum (Fig. 2b inset). In addition, Raman spectra of both PEDOT film and PEDOT-QDs are similar and in agreement with the characteristic spectrum of PEDOT[22] (Figure 2d). Consistent with XPS characterization, Fourier transform infrared spectra (FTIR) of PEDOT-QDs (Figure 2e) in both water and DMF show the characteristic peaks from PEDOT at 1638 cm^{-1} (C=C stretching vibration), 1385 cm^{-1} (C=C stretching of thiophene ring), 1124 cm^{-1} (polythiophene absorption), 1084 cm^{-1}(C–O stretching), and 929 cm^{-1} (C–S stretching)[23]. And the peaks from $BMIMBF_4$ are also observed at 1576 cm^{-1} and 1459 cm^{-1} (both from imidazole ring adsorption) [24]. The d_{020} peak in the X-ray diffraction (XRD) spectrum of PEDOT film or PEDOT-QDs corresponds to the face-to-face packing between the PEDOT chains with a distance of 0.34 nm[17] (Figure 2f). This correlates well with the HRTEM observation shown in Figure 1d.

A simple method for synthesis of a new type of polymer QDs is demonstrated. In addition to mechanical stress introduced by sonication, it is conceivable that exfoliation of QDs from PEDOT fibers is also facilitated by the intercalation of $BMIMBF_4$. The imidazole ring of $BMIM^+$ may interact with PEDOT *via* pi-pi and electrostatic interactions. In support of this, it has been previously reported that ionic liquids can intercalate into PEDOT films and cause swelling[25]. Furthermore, it seems that the DMF solvent also plays an important role in exfoliation and stabilizing the exfoliated QDs. In comparison, high-yield exfoliation of QDs does not occur in other solvents (specifically, ethanol, water, and acetonitrile).

Optical characterizations of PEDOT-QDs.

The as-prepared QDs are well dispersed in DMF. They can be extracted using rotary evaporation and re-suspended in water. The absorption spectra of these two suspensions are shown in Figure 3a. The water suspension of QDs efficiently absorbs UV light while the DMF suspension extends its adsorption to visible light region. The excitation-dependent emission spectra of both QD suspensions indicate the maximum emission peaks from PEDOT-QDs in DMF and in water at 533 nm (excited at 460 nm) and 450 nm (excited at 360 nm), respectively (Figure 3b,c). Clearly, the optical properties of PEDOT-QDs depend on their

interaction with the solvent. And the excitation dependence suggests the heterogeneity in size and properties of synthesized QDs. In comparison, EDOT monomers suspended in DMF or water don't show apparent absorption and emission, suggesting that the observed optical properties arise from the confined conjugation of these monomers.

To reveal the absorption and emission mechanism, density functional theory (DFT) and time-dependent DFT (TDDFT) calculations are performed. The DFT calculations on EDOT trimers (using it as a model compound for PEDOT-QDs) suggest that they can assume three possible configurations (isomer 1 – 3 as shown in Figure S1, ESI). Isomer 3, which has high dipole moment, is most thermodynamically stable in water by forming multiple hydrogen bonds with water molecules, but not in aprotic DMF solvent. Therefore, we speculate that DMF suspension contains isomer 1 and 2 while water suspension only has isomer 3. Theoretical calculations show that the absorption peaks of isomer 1 and 2 in the dielectric environment of DMF are 411 and 390 nm, respectively (Table 1, ESI). These values agree well with the experimentally observed peaks at ~412 nm and ~384 nm (Figure 3a). The absorption peak of isomer 3 in water is predicted to be 362 nm which is also close to the experimental observation (~360 nm as shown in Figure 3a). Similar to the observed emission peak of PEDOT-QDs in DMF (~533 nm), the emission peaks of isomer 1 and 2 are calculated to be 515 and 523 nm, respectively (Table 2, ESI). Isomer 3 in water is predicted to emit at 477 nm, consistent with observed emission peak of PEDOT-QDs in water (~450 nm).

PEDOT is natively non-fluorescent due to small optical band-gap (1.6 eV) which leads to rapid electron-hole recombination[26]. As shown by our theoretical studies (Table 1, ESI), the resulting photoluminescence properties of the nano-sized PEDOT-QDs arise from the band-gap widening due to quantum confinement. The PEDOT-QDs exhibit two excitation peaks (Figure S2, ESI) resulting from σ to π^* and π to π^* transitions (Figure S3, ESI).

Organic fluorophores, such as FITC, bleach quickly under confocal imaging (Figure 3d). Remarkably, no bleaching was observed from both PEDOT-QDs after long-term imaging. Intriguingly, the green QDs (in DMF) significantly increase the fluorescence intensity under illumination. Furthermore, the photo-bleaching studies performed over 2 hours using a spectro-fluorometer indicate a similar behavior except that the PL of blue QDs decreases slightly (Figure S4, ESI). It is conceivable that laser annealing further improves the crystalline structure of PEDOT-QDs[27-29]. The green QDs in DMF and blue QDs in water have a quantum yield of 13% (using Rhodamine 6G as the reference) and 4% (using quinine sulfate as the reference), respectively.

Furthermore, the two-photon excited photoluminescence (TPPL) of our PEDOT-QDs was examined. TPPL offers unique advantages over the conventional one-photon excitation, including larger penetration depth into the tissue and higher signal-to-noise ratio benefiting from the longer excitation wavelength and nonlinear absorption process[30]. The PEDOT-QDs exhibit strong emission under two-photo excitation (800 nm, even at a relatively low intensity of 6.7 GW/cm^2) (Figure S5a, ESI). The two-photon excitation process is clearly evidenced by the nearly quadratic excitation intensity dependence of the PL signals in the corresponding log-log plot of the PL signals versus excitation intensity [31](Figure S5b, ESI). An outstanding photostabilty under two-photon excitation is demonstrated with the retention of >90% of the initial emission after ~50 min, when operated at a pumping intensity of 20.1 GW/cm^2 (Figure S5c, ESI). The molecular size and remarkable photo-stability of PEDOT-QDs under both single and two-photon excitation promise their applications for bio-imaging. Furthermore, a high concentration (150 μg/mL) of PEDOT-QDs is not able to induce significant cytotoxicity, indicating good biocompatibility of these QDs (Figure S6, ESI).

Cellular Imaging using PEDOT-QDs

Interestingly, diluting the DMF-suspended QDs in water (95% dilution), their green fluorescence properties preserve suggesting the persistent association between DMF molecules and PEDOT-QDs (Figure S7, ESI). As the proof-of-concept demonstration for cellular imaging, we incubated PC12 cells with blue water-suspended QDs (76.6 μg/mL) and DMF-associated green QDs diluted in cell culture medium (5.5 μg/mL) for 24 hr. As shown in Figure 4, both types of PEDOT-QDs are up-taken into the cells and remain fluorescent. Some QDs are located in the early endosomes which are specifically labeled by the fluorescent early endosome marker (mRFP-Rab5).

Optical detection of mercury ions (Hg^{2+}) using PEDOT-QDs

Similar to other synthetic quantum dots[8,9,32], the small PEDOT-QDs promise wide applications in optical sensing. As the proof-of-concept demonstration, we show here that the photoluminescence (PL) of PEDOT-QDs can be significantly quenched by 57% upon addition of 100 μM Hg^{2+} ions whereas the PEDOT-QDs are not obviously responsive to other metal ions (Pb^{2+}, Zn^{2+}, Cd^{2+}, Cs^{+}, Mg^{2+}, Co^{2+}, Ni^{2+}, Mn^{2+}, K^{+} and Au^{3+}) (Figure 5a). PL quenching by Hg^{2+} is dose-dependent (Figure 5b). And as shown in Fig. 6c, the extrapolated lower theoretical detection limit is as low as 0.87 μM (with S/N = 3) and the linear response is up to 10 μM.

It has been previously reported that nitrogen-containing imidazole[33] and sulfur-containing thiophene[34] can bind with Hg^{2+} with high affinity. Therefore, Hg^{2+} ions act as a coordinating center to bridge several PEDOT-QDs together, by interacting with thiophene groups from PEDOT and imidazole groups from BMIM associated with PEDOT-QD *via* pi-pi interactions. In turn, fluorescence quenching occurs due to aggregation of QDs. Indeed, Hg^{2+}-induced QD aggregations are observed under AFM (Figure S8, ESI).

Conclusions

In conclusion, we have developed a facile and general strategy to synthesize novel fluorescent polymer quantum dots derived from non-fluorescent PEDOT. Such molecularly light, perfectly photo-stable PEDOT-QDs promise a wide range of applications in bio-imaging (e.g., single molecule tracking in live cells) and sensitive optical detection. In principle, the synthetic route demonstrated here can be easily modified (e.g., using different polymer precursors, ionic liquids for polymerization, solvents) to produce different types of polymer QDs with various interesting properties (preliminary results obtained).

Acknowledgements

This work was supported by the Singapore Ministry of Education under the AcRF Tier 2 grant (MOE2011-T2-2-010), NNSF of China (21275076, 61328401), Jiangsu Provincial Funds for Distinguished Young Scholars (SK20130046). We would also like to acknowledge the assistance from Arundithi Ananthanarayanan, Dr Parimal Routh, Chew Huai Ping and Xu Qian during sample synthesis, for sample preparation and discussion.

Notes

[a]*Division of Bioengineering, School of Chemical and Biomedical Engineering, Nanyang Technological University, 70 Nanyang Drive, 637457, Singapore. Email: chenpeng@ntu.edu.sg*
[b]*Division of Physics and Applied Physics, School of Physical and Mathematical Sciences , Nanyang Technological University, 21 Nanyang Link, 637371, Singapore.*
[c]*Jiangsu-Singapore Joint Research Center for Organic/Bio-Electronics & Information Displays and Institute of Advanced Materials (IAM), Nanjing Tech University, 30 South Puzhu Road, Nanjing 211816, China.*

† Electronic Supplementary Information (ESI) available: [details of any supplementary information available should be included here]. See DOI: 10.1039/b000000x/

References

1. I. L. Medintz, H. T. Uyeda, E. R. Goldman and H. Mattoussi, *Nat. Mater.*, 2005, **4**, 435-446.
2. D. Bera, L. Qian, T. K. Tseng and P. H. Holloway, *Materials*, 2010, **3**, 2260-2345.
3. A. M. Derfus, W. C. W. Chan and S. N. Bhatia, *Nano Lett.*, 2003, **4**, 11-18.
4. X. T. Zheng, A. Than, A. Ananthanaraya, D. H. Kim and P. Chen, *ACS nano*, 2013, **7**, 6278-6286.
5. L. Li, G. Wu, G. Yang, J. Peng, J. Zhao and J. J. Zhu, *Nanoscale*, 2013, **5**, 4015-4039.
6. H. J. Sun, L. Wu, W. L. Wei and X. G. Qu, *Mater. Today*, 2013, **16**, 433-442.
7. R. Freeman and I. Willner, *Chem. Soc. Rev.*, 2012, **41**, 4067-4085.
8. Y. Lou, Y. Zhao, J. Chen and J.-J. Zhu, *J. Mater. Chem. C*, 2014, **2**, 595.
9. A. Ananthanarayanan, X. Wang, P. Routh, B. Sana, S. Lim, D.-H. Kim, K.-H. Lim, J. Li and P. Chen, *Adv. Funct. Mater.*, 2014, doi:10.1002/adfm.201303441.
10. X. Zhang, J. Yu, Y. Rong, F. Ye, D. T. Chiu and K. Uvdal, *Chem. Sci.*, 2013, **4**, 2143.
11. C. Wu, C. Szymanski, Z. Cain and J. McNeill, *J. Am. Chem. Soc.*, 2007, **129**, 12904-12905.
12. C. Wu, Y. Jin, T. Schneider, D. R. Burnham, P. B. Smith and D. T. Chiu, *Angew. Chem., Int. Ed.*, 2010, **49**, 9436-9440.
13. C. Wu and D. T. Chiu, *Angew. Chem., Int. Ed.*, 2013, **52**, 3086-3109.
14. Z. Tian, J. Yu, C. Wu, C. Szymanski and J. McNeill, *Nanoscale*, 2010, **2**, 1999-2011.
15. T. Kietzke, D. Neher, K. Landfester, R. Montenegro, R. Guntner and U. Scherf, *Nat. Mater.*, 2003, **2**, 408-412.
16. Y. Chen, P. P. Gai, L. Jin, D. Zhu, D. B. Tian, E. S. Abdel-Halim, J. R. Zhang and J. J. Zhu, *J. Mater. Chem. B*, 2013, **1**, 3451-3457.
17. D. C. Martin, J. Wu, C. M. Shaw, Z. King, S. A. Spanninga, S. Richardson-Burns, J. Hendricks and J. Yang, *Polym. Rev.*, 2010, **50**, 340-384.
18. S. Bhandari, M. Deepa, S. Singh, G. Gupta and R. Kant, *Electrochim. Acta*, 2008, **53**, 3189-3199.
19. Y. Yao, N. Liu, M. T. McDowell, M. Pasta and Y. Cui, *Energy Environ. Sci.*, 2012, **5**, 7927.
20. K. Kinoshita, N. Matsunaga, M. Hiraoka, H. Yanagimoto and H. Minami, *RSC Adv.*, 2014, **4**, 8605.
21. H. J. Kim, I. S. Bae, S. J. Cho, J. H. Boo, B. C. Lee, J. Heo, I. Chung and B. Hong, *Nanoscale Res. Lett.*, 2012, **7**, 30.
22. X. Zhang, D. Chang, J. Liu and Y. Luo, *J.Mater. Chem.*, 2010, **20**, 5080.
23. D. Sun, L. Jin, Y. Chen, J. R. Zhang and J. J. Zhu, *Chempluschem*, 2013, **78**, 227-234.
24. N. Xie and W. Luan, *Nanotechnology*, 2011, **22**, 265609.
25. V. Armel, J. Rivnay, G. Malliaras and B. Winther-Jensen, *J.Am. Chem. Soc.*, 2013, **135**, 11309-11313.
26. A. Elschner, S. Kirchmeyer, W. Lovenich, U. Merker and R. K, *PEDOT : principles and applications of an intrinsically conductive polymer*, CRC Press, Boca Raton, FL, 2011.
27. J. J. Dubowski, C. N. Allen and S. Fafard, *Appl. Phys. Lett.*, 2000, **77**, 3583.
28. S. Chakrabarti, S. Fathpour, K. Moazzami, J. Phillips, Y. Lei, N. Browning and P. Bhattacharya, *J. Electron. Mater.*, 2004, **33**, L5-L8.
29. X. Li, H. Wang, Y. Shimizu, A. Pyatenko, K. Kawaguchi and N. Koshizaki, *Chem. Comm.*, 2011, **47**, 932-934.
30. G. S. He, L. S. Tan, Q. Zheng and P. N. Prasad, *Chem. Rev.*, 2008, **108**, 1245-1330.
31. Y. Wang, X. Yang, T. C. He, Y. Gao, H. V. Demir, X. W. Sun and H. D. Sun, *Appl. Phys. Lett.*, 2013, **102**, 021917.
32. X. Ran, H. Sun, F. Pu, J. Ren and X. Qu, *Chem. Comm.*, 2013, **49**, 1079-1081.
33. S. Madhu, D. K. Sharma, S. K. Basu, S. Jadhav, A. Chowdhury and M. Ravikanth, *Inorg. Chem.*, 2013, **52**, 11136-11145.
34. A. Pal and B. Bag, *J. Photochem. Photobiol., A*, 2012, **240**, 42-49.

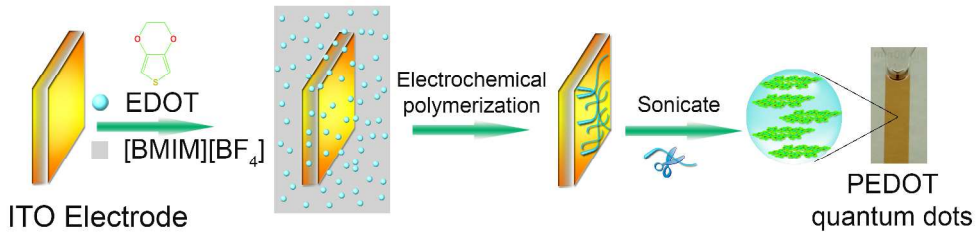

Scheme 1. Schematic illustration for the preparation of PEDOT-QDs.

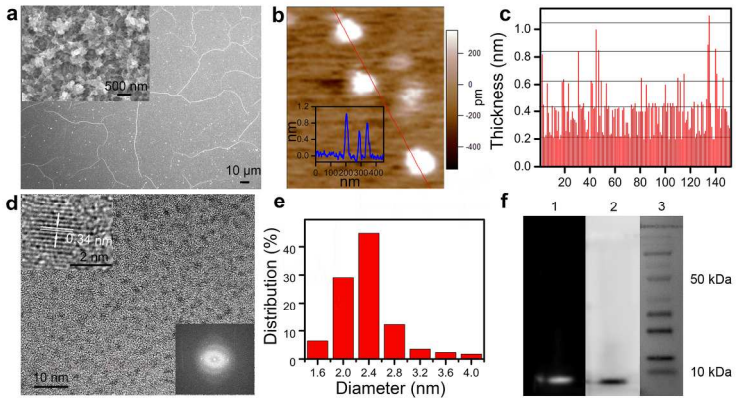

Figure 1. QDs exfoliated from the fibrous electropolymerized PEDOT film are small and uniform in size. (a) FESEM image of the PEDOT. Inset shows the film surface with a higher-resolution. (b) AFM image of PEDOT-QDs. Inset shows the height profile along the indicated line. (c) The height (thickness) of 152 individual QDs. The indicative horizontal lines are 0.21 nm apart. (d) HRTEM image of PEDOT-QDs. The upper inset presents a single QD with crystal lattice resolved. The lower inset gives the FTT diffraction pattern. (e) Diameter distribution of 172 QDs. (f) The gel electrophoresis of PEDOT-QDs (1 - fluorescent image under UV; 2 – bright field image) and protein markers (3).

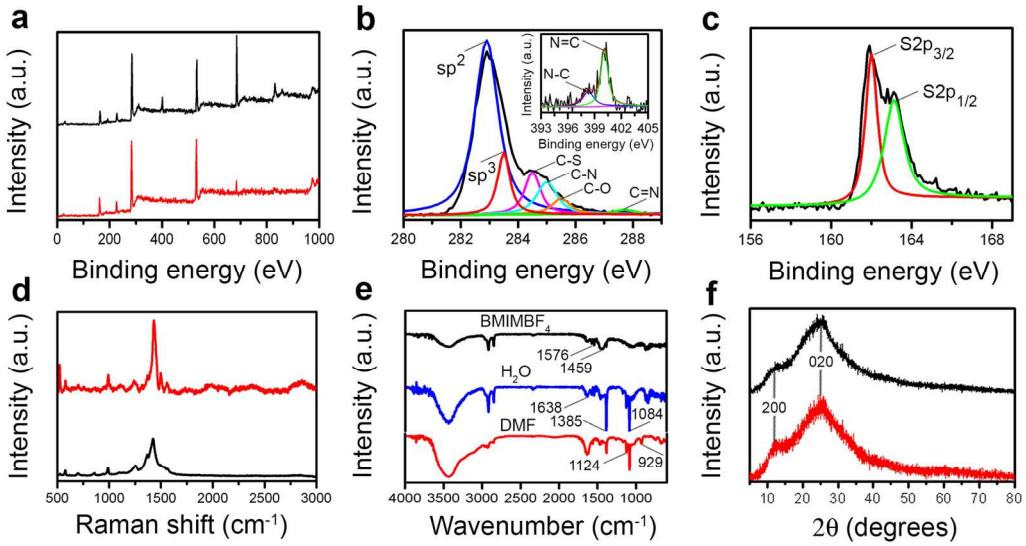

Figure 2. **Spectroscopic characterizations. (a)** XPS spectra of PEDOT film (black) and PEDOT-QDs (red). **(b)** High-resolution C1s peak in XPS spectrum of PEDOT QDS. Inset shows N1s peak. **(c)** High-resolution S2p peak in XPS spectrum of PEDOT QDs. **(d)** Raman spectra of PEDOT film (black) and PEDOT-QDs (red). **(e)** FTIR spectra of $BMIMBF_4$ (black), PEDOT-QDs (blue – in water; red – in DMF). **(f)** XRD Spectra of PEDOT Film (black) and PEDOT QDs (red).

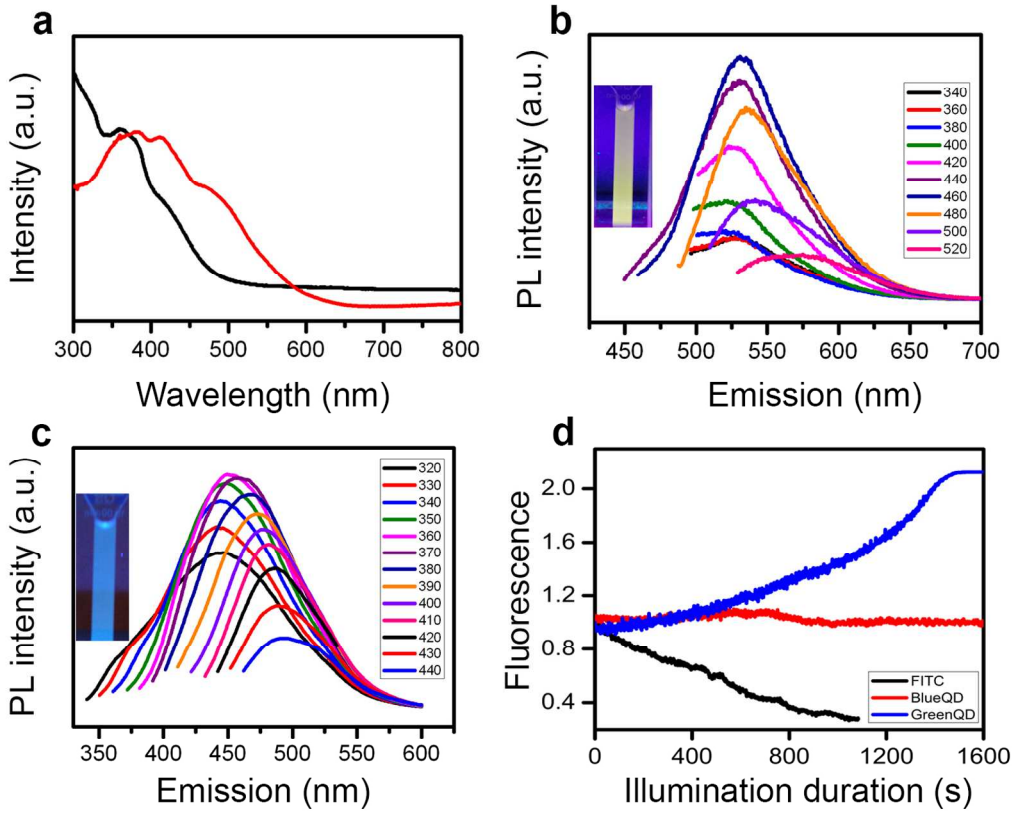

Figure 3. Optical characteristics of PEDOT-QDs. (a) UV-vis adsorption spectrum of PEDOT QDs in water (black) and DMF (red). **(b)** and **(c)** PL spectra of QDs in DMF and water with different excitation wavelengths. The insets show the images of the QD suspensions under UV. **(d)** The photobleaching behavior showing normalized fluorescence of the green QDs (in DMF), blue QDs (in water), and FITC under continuous confocal imaging.

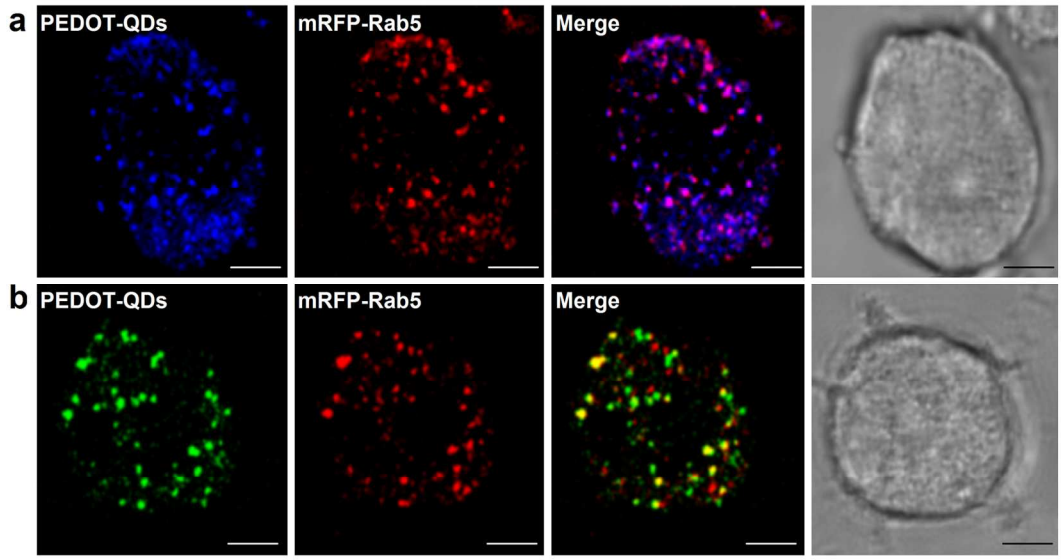

Figure 4. Confocal imaging of PC12 cells after incubation with blue (a) or green (b) PEDOT-QDs. Confocal images with staining of QDs (column 1), endosome marker mRFP-Rab5 (column 2). Column 3 is the merged image of column 1 and 2. Column 4 shows the bright-field image of the cells. Scale bar = 5 μ m.

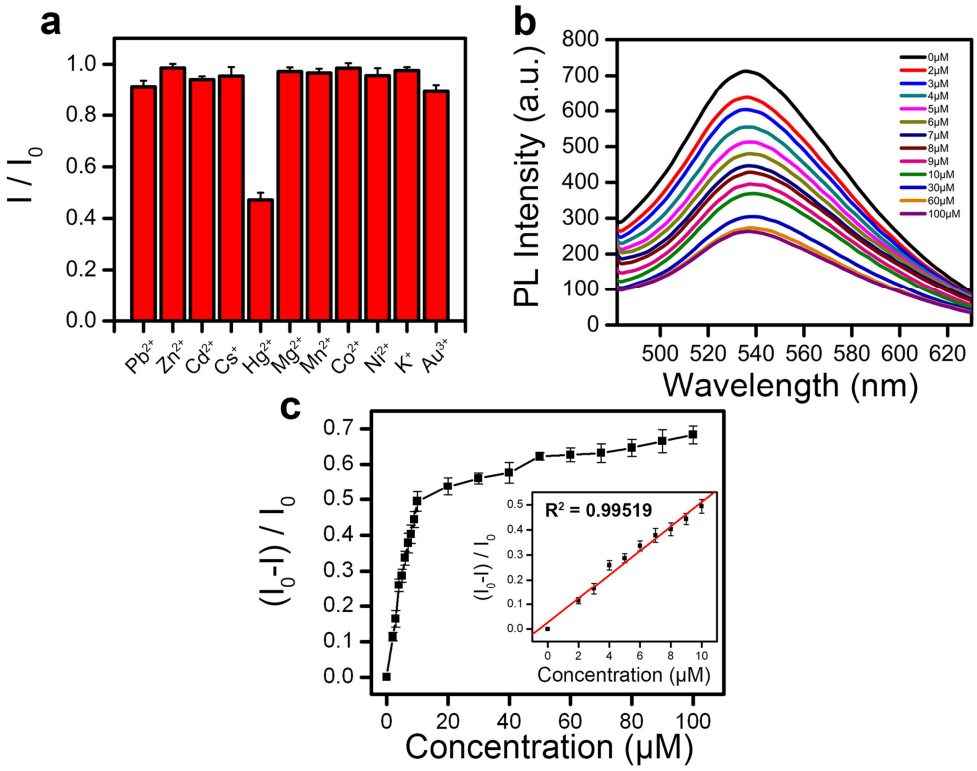

Figure 5. Sensitive and selective optical detection of Hg^{2+} ions. (a) PL of PEDOT-QDs (200 μg/mL in water) is selectively quenched by Hg^{2+} (100 μM), but not other metal ions at the concentration **(b)** The PL emission spectra of PEDOT-QDs with various concentrations of Hg^{2+} **(c)** The relative concentration-dependent fluorescence response of PEDOT-QDs. Inset shows the linear response range. The error bars represent the standard deviation of the measurements from three different samples.

Graphic Abstract

Fluorescent polymer quantum dots derived from poly(3,4-ethylenedioxythiophene) are synthesized, and utilized for optical imaging and Hg^{2+} sensing applications.

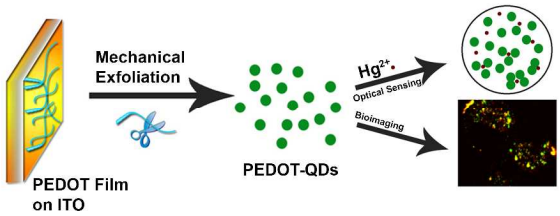

Conceptual Insights

Due to the intrinsic limitations suffered by the current fluorophores (e.g., fluorescent proteins, organic dyes, and semiconductor quantum dots), seeking better fluorescent reporters which are photostable, biocompatible, and of molecular size is an ongoing and critical effort for the areas of bioimaging and optical sensing. We herein report a facile and general approach to synthesize novel polymer-based quantum dots (QDs). Furthermore, as the proof-of-concept demonstration, such new type of QDs is used for cellular imaging and sensitive optical detection of mercury ions.